Better-Than-Chance Classification for Signal Detection

Jonathan Rosenblatt   Roee Gilron   Roy Mukamel

August 11, 2016

1   **Abstract**

2   [TODO]

1   Introduction

4   A common workflow in neuroimaging consists of fitting a classifier, and es-
5   timating its predictive accuracy using cross validation. Given that the cross
6   validated accuracy is a random quantity, it is then common to test if the
7   cross validated accuracy is significantly better than chance using a permu-
8   tation test. Examples in the neuroscientific literature include Golland and
9   Fischl [2003], Pereira et al. [2009], Varoquaux et al. [2016], and especially
10 the recently popularized *multivariate pattern analysis* (MVPA) framework
11 of Kriegeskorte et al. [2006]. This practice is also observed in very high pro-
12 file publications in the genetics literature: Golub et al. [1999], Slonim et al.
13 [2000], Radmacher et al. [2002], Mukherjee et al. [2003], Juan and Iba [2004],
14 Jiang et al. [2008].

15   To fix ideas, we will adhere to a concrete example. In Gilron et al. [2016],
16 the authors seek to detect brain regions which encode differences between
17 vocal and non-vocal stimuli. Following the MVPA workflow, the localization
18 problem is cast as a supervised learning problem: if the type of the stimulus
19 can be predicted from the spatial activation pattern significantly better than
20 chance, then a region is declared to encode vocal/non-vocal information. We
21 call this an *accuracy test*, a.k.a. *class prediction*, or *pattern discrimination*

22   This same signal detection task can be also approached as a two-group
23 multivariate test. Inferring that a region encodes vocal/non-vocal informa-
24 tion, is essentially inferring that the spatial distribution of brain activations
25 is different given a vocal/non-vocal stimulus. As put in Pereira et al. [2009]:

26   ... the problem of deciding whether the classifier learned to dis-
27   criminate the classes can be subsumed into the more general ques-
28   tion as to whether there is evidence that the underlying distribu-
29   tions of each class are equal or not.

30 A practitioner may then call upon a two-group population test such as
31 Hotelling's T^2 [Anderson, 2003]. Alternatively, if the size of a brain re-
32 gion is large compared to the number of observations, so that the spatial
33 covariance cannot be fully estimated, then a high dimensional version of
34 Hotelling's test can be called upon, such as in Schäfer and Strimmer [2005]
35 or Srivastava [2007]. For brevity, and in contrast to *accuracy tests*, we will
36 call any two-sample multivariate tests simply *population tests*, also termed
37 *class comparisons*. [TODO: rename to parameter test?]
38   At this point, it becomes unclear which is preferable: a population test or
39 an accuracy test? The former with a heritage dating back to Hotelling [1931],
40 and the latter being extremely popular, as the 959 citations[1] of Kriegeskorte
41 et al. [2006] suggest.
42   The comparison between location and accuracy tests was precisely the
43 goal of Ramdas et al. [2016], who compared the T^2 population test to the
44 accuracy of *Fisher's linear discriminant analysis* classifier (LDA). By com-
45 paring the rates of convergence of the powers to 1, Ramdas et al. [2016]
46 concluded that accuracy and population tests are rate equivalent.
47   Asymptotic relative efficiency measures (ARE) are typically used by statis-
48 ticians to compare between rate-equivalent test statistics [van der Vaart,
49 1998]. Ramdas et al. [2016] derive the asymptotic power functions of the
50 two test statistics, which allows to compute the ARE between Hotelling's T^2
51 (location) test and Fisher's LDA (accuracy) test. Theorem 14.7 of van der
52 Vaart [1998] relates asymptotic power functions to ARE. Using the results of
53 Ramdas et al. [2016] we deduce that the ARE is lower bounded by $2\pi \approx 6.3$.
54 This means that Fisher's LDA requires at least 6.3 more samples to achieve
55 the same (asymptotic) power than the T^2 test. In this light, the accuracy
56 test is remarkably inefficient compared to the population test. For compar-
57 ison, the t-test is only 1.04 more (asymptotically) efficient than Wilcoxon's
58 rank-sum test [Lehmann, 2009], so that an ARE of 6.3 is strong evidence in
59 favor of the population test.
60   Before discarding accuracy tests as inefficient, we recall that Ramdas
61 et al. [2016] analyzed a *half-sample* holdout. The authors conjectured that a
62 leave-one-out approach, which makes more efficient use of the data, may have
63 better performance. Also, the analysis in Ramdas et al. [2016] is asymptotic.
64 This eschews the discrete nature of the accuracy statistic, which will be

---

[1]GoogleScholar. Accessed on Aug 4, 2016.

shown to have crucial impact. Since typical sample sizes in neuroscience are not large, we seek to study which test is to be preferred in finite samples? Our conclusion will be quite simple: *population tests almost always have more power than accuracy tests*.

Our statement rests upon the observation that with typical sample sizes, the accuracy test statistic is highly discrete. Permutation testing with discrete test statistics are known to be conservative [Hemerik and Goeman, 2014], since they are insensitive to mild perturbations of the data, and they cannot exhaust the permissible false positive rate. The degree of discretization is governed by the number of samples. In our neuroscience example from Gilron et al. [2016], the classification is performed based on 40 trials, so that the test statistic may assume only 40 possible values. This number of examples is not unusual if considering this is the number of trial-repeats, or the number of subjects in an neuroimaging study.

The discretization effect is aggravated if the test statistic is highly concentrated. For an intuition consider the usage of a the *resubstitution accuracy* as a test statistic. This statistic simply means that the accuracy is not cross validated. If the data is high dimensional, the resubstitution accuracy will be very high due to over fitting. In a very high dimensional model, the resubstitution accuracy will be 1 for the observed data [McLachlan, 1976, Theorem 1], but also for any permutation. The concentration of resubstitution accuracy near 1, and its discreteness, render this test completely useless, with a power tending to 0 for any (fixed) effect size, as the dimension of the model grows.

To compare the power of accuracy tests and population tests in finite samples, we perform a simulation study of a battery of test statistics. We start with fomalizing the problem in Section 2. The main findings are reported in Sections 4 and 5. A discussion follows in Section 6.

2   Problem setup

Let $y \in \mathcal{Y}$ be a class encoding. Let $x \in \mathcal{X}$ be a p dimensional feature vector. In our vocal/non-vocal example we have $\mathcal{Y} = \{-1, 1\}$ and p, the number of voxels in a brain region so that $\mathcal{X} = \mathbb{R}^{27}$.

Given n pairs of (x_i, y_i), typically assumed i.i.d., a population test amounts to testing whether $x|y = 1$ has the the same distribution as $x|y = -1$. I.e., we test if the multivariate voxel activation pattern has the same distribution when given a vocal stimulus, as when given a non-vocal stimulus.

An accuracy test amounts to learning a predictive model $\hat{f}(x)$ from some assumed model class $\hat{f} \in \mathcal{F}$. The prediction accuracy, denoted $\mathcal{E}_{\hat{f}}$, is de-

fined as the probability of a given classifier $\hat{f}$ of making a correct prediction. Denoting by $I(A)$ the indicator function of the event A, we have $\mathcal{E}_{\hat{f}} := \mathbf{E}\left[I(\hat{f}(x) = y)\right]$ when given a randomly drawn data point, (x, y). A statistically significant "better than chance" estimate of $\mathcal{E}_{\hat{f}}$ is evidence that the classes are distinct.

2.1 Candidate Tests

The design of a permutation test using the prediction accuracy, requires the following design choices:

1. Is the statistic cross validated or not?

2. For a V-fold cross validated test statistic:

    (a) Should the data be refolded in each permutation?

    (b) Should the data folding be balanced (a.k.a. stratified)?

    (c) How many folds?

3. How to estimate accuracy?

We will now address these questions while bearing in mind that unlike the typical supervised learning setup, we are not interested in an unbiased estimate of the prediction error, but rather in the mere detection of a difference between two groups.

Cross validate or not? Since we are merely interested in detecting a difference between classes, a biased error estimate is not an issue provided that bias is consistent over all permutations. The underlying intuition is that if the exact same computation is performed over all permutations, then a permutation test will be "fair", i.e., will not inflate the false positive rate. We will thus be considering both cross validated accuracies, and resubstitution accuracies as our test statistics.

Balanced folding? The standard practice when cross validating is to constrain the data folds to be balanced (i.e. stratified) [e.g. Ojala and Garriga, 2010]. We will report results with both balanced and unbalanced data foldings, only to discover, it does not really matter.

Refolding? The standard practice in neuroimaging is to refold the data after each permutation, so that data folds are balanced after each label permutation. We will adhere, even though it can be circumvented by permuting features instead of labels, as done by Golland et al. [2005].

How many folds? Different authors suggest different rules for the number of folds. We will be varying the number of folds, and ultimately discover that the power *decreases with the number of folds*.

How to estimate accuracy? Given a predictor $\hat{f}$, a natural test statistic is some estimate of its accuracy $\mathcal{E}_{\hat{f}}$. Complicating matters: very low accuracies, even 0, is evidence that the classes are separated, and we only need to invert the predictions. We can thus consider $|\mathcal{E}_{\hat{f}} - 0.5|$ as the test statistic. This, however, implies that if the classes are identical, random guessing has 0.5 accuracy. This is not true if the classes are not balanced. For unbalanced data the accuracy chance level is the probability of the majority class, we denote by $\hat{p}_{max}$ [Golland et al., 2005, Sec 4.1]. This suggests the following test statistic $|\mathcal{E}_{\hat{f}} - \hat{p}_{max}|$. Since we will be aggregating these statistics over random data sets where $\hat{p}_{max}$ may vary, it seems appropriate to standardize the scale of this statistic. We thus also consider the z-scored accuracy: $|\mathcal{E}_{\hat{f}} - \hat{p}_{max}|/\sqrt{\hat{p}_{max}(1 - \hat{p}_{max})}$.

The of tests we will be comparing is collected for convenience in Table 1.

| Name	Basis	CV	Accuracy	Parameters
Hotelling	Hotelling	–	–	shrink=FALSE
Hotelling.shrink	Hotelling	–	–	shrink=TRUE
lda.CV.1	LDA	TRUE	accuracy	–
lda.CV.2	LDA	TRUE	z-accuracy	–
lda.noCV.1	LDA	FALSE	accuracy	–
lda.noCV.2	LDA	FALSE	z-accuracy	–
sd	SD	–	–	–
svm.CV.1	SVM	TRUE	accuracy	cost=1e1
svm.CV.2	SVM	TRUE	accuracy	cost=1e-1
svm.CV.3	SVM	TRUE	z-accuracy	cost=1e1
svm.CV.4	SVM	TRUE	z-accuracy	cost=1e-1
svm.noCV.1	SVM	FALSE	accuracy	cost=1e1
svm.noCV.2	SVM	FALSE	accuracy	cost=1e-1
svm.noCV.3	SVM	FALSE	z-accuracy	cost=1e1
svm.noCV.4	SVM	FALSE	z-accuracy	cost=1e-1

Table 1: This table enumerates the various test statistics we will be studying. Three are population tests: Hotelling, Hotelling.shrink, and sd. *Hotelling* is the classical two-group T^2 statistic. *Hotelling.shrink* is a high dimensional version with the regularized covariance in Schäfer and Strimmer [2005]. *sd* is another high dimensional version of the T^2, from Srivastava et al. [2013]. The rest of the tests are variations of the linear SVM, and Fisher's LDA, with varying accuracy measures, cross validated or not, and varying tuning parameters. For example, *svm.CV.4* is a linear SVM, with *libsvm*'s cost parameter set at 0.1, using the cross validated z-scored accuracy ($|\mathcal{E}_{\hat{f}} - \hat{p}_{max}/\sqrt{\hat{p}_{max}(1 - \hat{p}_{max})}$, see Section 2.1). Another example is *lda.noCV.1*, which is Fisher's LDA, returning the resubstitution accuracy, without cross validation, and without z-scoring.

3 Controlling the False Positive Rate

Figure 1 demonstrates that all of the tests considered conserve the desired 0.05 false positive rate, up to varying levels of conservativism. This can be seen from the fact that the probability of rejection is no larger than 0.05 in the absence of any effect, encoded by a red circle. This is true, in particular if: (a) the folds are balanced or not, (b) the tuning parameters of some test statistic are varied, (d) the number of folds is varied. We also observe that the most conservative tests are the resubstitution accuracy measures. We return to this matter in the Discussion.

Figure 1: The power of a permutation test with various test statistics. The power on the x axis. Effect are color and shape coded. The various statistics on the y axis. Their details are given in Table 1. Effects vary over 0 (red circle), 0.25 (green triangle), and 0.5 (blue square). Simulation details in Appendix B. Cross-validation was performed with balanced (stratified) and unbalanced data folding. See sub-captions.

(a) Unbalanced.　　　　　**(b) Balanced.**
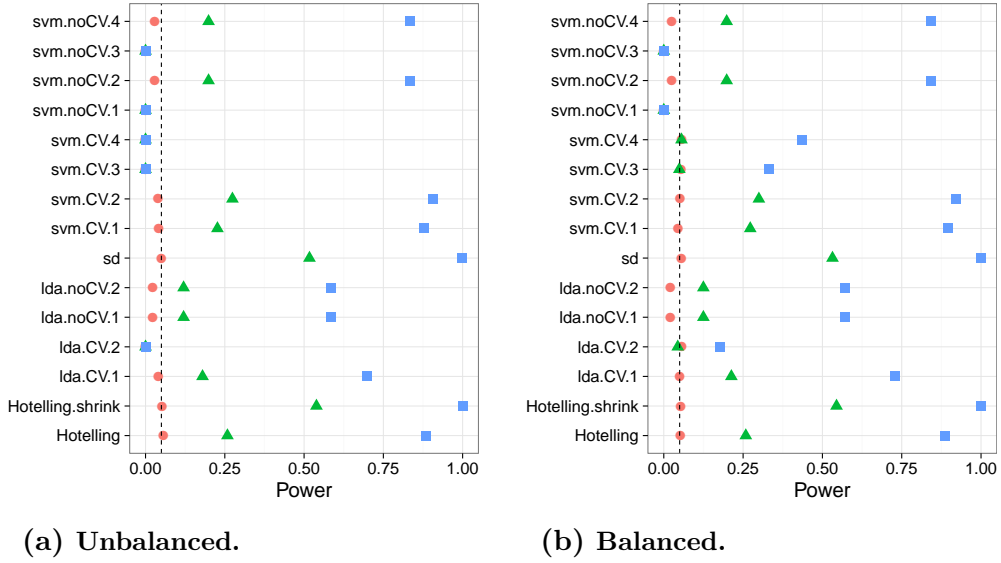
4 Power

Having established that all of the tests in our battery control the false positive rate, it remains to be seen if they have similar power– especially when comparing the power of population tests to accuracy tests. From the simulation results reported in Appendix C we collect the following insights:

1. population tests have more power than accuracy tests in all our configurations.

2. The conservativeness decays as the sample grows (Figures 8a, 8b and 9a), suggesting that concentration and/or discretization is responsible for power loss.

3. The power may increase or decrease with the number of folds (Figure 5).

4. The z-scoring of the accuracies was introduced to deal with unbalanced foldings. If the z-scoring has any effect at all, it merely kills power. There is really no reason to use it.

7

5. Both accuracy and population tests are inappropriate for scale alternatives (Figure 7a). This was to be expected and is reported mostly as a sanity check.

6. The presence of heavy tails (Figure 7b) may reduce power, but does not quantitatively change results.

7. Balanced folding typically has no effect. It increased power only for the z-scored statistics (Figure 1). This is surprising given they were precisely designed to deal with the presence of imbalance.

8. Varying the accuracy test's tunning parameter, such as the cost (i.e. margins) has no effect on the power of the test.

9. Correlation between coordinates, mimicking temporal correlation in fMRI data, has no effect on conclusions, since all test statistics account for this correlation (Figure 9b).

The major insight from simulations is that the use of accuracy tests for signal detection is underpowered compared to population tests. We now verify this finding on a neuroimaging dataset.

5 Neuroimaging Example

Figure 2 is an application of both a location and an accuracy test to the data of Pernet et al. [2015]. The authors of Pernet et al. [2015] collected fMRI data while subjects were exposed to the sounds of human speech (vocal), and other non-vocal sounds. Each subject was exposed to 20 sounds of each type, totaling in $n = 40$ trials in each scan. The study was rather large and consisted of about 200 subjects. The data was kindly made available by the authors at the OpenfMRI website[2].

We perform group inference using within-subject permutations using the pipeline of Stelzer et al. [2013], which was also reported in Gilron et al. [2016]. For completeness, the pipeline is described in Appendix A. To demonstrate our point, we compare the *sd* population test with the *svm.cv.1* accuracy test (see Table 1 for the definition of these statistics).

In agreement with our simulation results, the population test (*sd*) discovers more brain regions when compared to an accuracy test (*svm.cv.1*). The former discovers $1,232$ regions, while the latter only 441, as depicted in Figure 2. We emphasize that both test statistics were compared with the same

---

[2]https://openfmri.org/

permutation scheme, and the same error controls, so that any difference in detections is due to their different power.

Having established that accuracy tests are underpowered both in simulation and in application, we wish to identify the conditions under which this will occur, and discuss implications on the practice of accuracy tests.
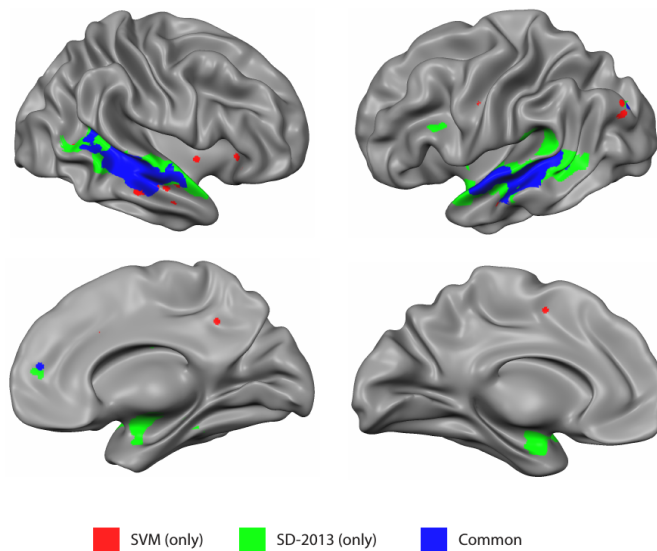

Figure 2: Brain regions encoding information discriminating between vocal and non-vocal stimuli. Map reports the centers of 27-voxel sized spherical regions, as discovered by an accuracy test (svm.cv.1), and a population test (sd). svm.cv.1 was computed using 5-fold cross validation, and a cost parameter of 1. Region-wise significance was determined using the permutation scheme of Stelzer et al. [2013], followed by region-wise FDR ≤ 0.05 control using the Benjamini-Hochberg procedure [Benjamini and Hochberg, 1995]. Number of permutations equals 400. The population test detect 1,232 regions, and the accuracy test 441,399 of which are common to both. For the details of the analysis see Appendix A and Gilron et al. [2016].

6   Discussion

We have set out to understand which of the tests is more powerful: the accuracy test or the population test. Using simulations, we have concluded that the population tests are preferable. Their high dimensional versions such as Srivastava [2007] and Schäfer and Strimmer [2005] are preferable for typical neuroimaging problems such as MVPA. We attribute this to several phenomena: (a) Discretization introduced in finite samples by the accuracy

9

test statistic. (b) Inefficient use of the data for the validation holdout set. The presence of heavy tails shrinks the power advantage of the population tests over accuracy tests.

The insensitivity of the power to the number of folds suggests that most of the power is lost due to the discretization and not to the holdoutsize. The degree of discretization is governed by the sample size. For this reason, an asymptotic analysis such as Ramdas et al. [2016] may uncover the holdout inefficiency, but will not uncover the discretization effect. The practical advice for the practitioner, is that for the purpose of signal detection, there is typically a multivariate test (be it a population test or other), that is more powerful than an accuracy test. There is also a good chance that it would be easier to implement, since no cross validation will be involved.

6.1   Ease of implementation

A very important consideration is the ease of implementation. The need for cross validation of the accuracy test greatly increases its computational complexity. Moreover, anyone who has actually implemented tests with discrete statistics, will attest they are more prone to programming errors. This is because their unforgiveness to the type of inequalities used. Indeed, mistakenly replacing a weak inequality with a strong inequality in one's program may considerably change the results. This is not the case for continuous test statistics.

6.2   A good accuracy test

In Section 6.6 we discuss cases where an accuracy test cannot replace a population test. For such cases we collect some conclusions from our simulations on the best practices for accuracy tests.

1. The conservativeness of accuracy tests decrease with sample size.

2. Permuting features is easier than permuting labels. It allows to preserve balanced folds after a permutation without refolding, thus reducing computational complexity.

3. For V-fold CV, it is unclear what is the effect of the number of folds. More folds increase power by reducing the number of holdout samples. On the other hand, it increases the concentration of the accuracy statistic. Compounded with the discreteness of the accuracy statistic, this decreases power. This suggests that the optimal number of folds may be problem specific.

4. Cross validating has no less power than resubstitution. The power loss due to the training sub-samples when cross validating, is smaller than the power loss due to the concentration of the resubstition statistic (Figure 8). For large sample sizes, discretization and concentration have weaker effects, so that the cross validated accuracy may be replaced with the computationally more efficiency resubstitution accuracy (Figure 9a). This also implies that there is a fundamental difference between V-folding and resubstitution, so that latter should not be thought of as the limit of the former.

5. There is no gain in z-scoring the accuracy scores. Our motivating rational was clearly flawed. [TODO: why?]

6. Cross validated accuracy with balanced folds has more power than unbalanced folds. [TODO: Why?].

7. The value of the tunning parameters of a classifier have little to no effect.

6.3 Smoothing accuracy estimates

It may be possible to alleviate the effect of discretization by appropriate cross-validation. The discreteness of the accuracy statistic can be "smoothed" by allowing the test sample to be drawn with replacement. The *bootstrap* may seem like a candidate approach, but since the original data always serves as a test set, the accuracy can still only assume $1/n$ values. This is not the case, however, for the *leave-one-out bootstrap estimator* (B-LOO) and the *0.632 bootstrap estimator* (B-0.632) [Hastie et al., 2003, Sec 7.11], which we define below for completeness. By the same rational, the degree of conservativism should decrease with the number of bootstrap samples.

Definition 1 (B-LOO). Denoting by $C^{(i)}$ the index set of bootstrap samples, b, where observation i is not in the train set, *leave-one-out bootstrap* estimate is defined as:

$$\mathcal{E}_{BLOO} := \frac{1}{n} \sum_{i=1}^{n} \frac{1}{|C^{(i)}|} \sum_{b \in C^{(i)}} I(\hat{f}^b(x_i) = y_i).$$

Equivalently, denoting by $S^{(b)}$ the indexes of observations, i, that are not in the bootstrap train sample b,

$$\mathcal{E}_{BLOO} := \frac{1}{B} \sum_{b=1}^{B} \frac{1}{|S^{(b)}|} \sum_{i \in S^{(b)}} I(\hat{f}^b(x_i) = y_i).$$

11

Definition 2 (B-0.632). Denoting by $\mathcal{E}_{resub}$ the resubstitution accuracy estimate, the B-0.632 accuracy estimator, $\mathcal{E}_{0.632}$, is defined as

$$\mathcal{E}_{0.632} := 0.368\,\mathcal{E}_{resub} + 0.632\,\mathcal{E}_{BLOO}.$$

The simlation results reported in Figure 3, with naming conventions in Table 2. It can be seen that selecting test sets with replacement does increase the power, when compared to V-fold cross validation, but still falls short from the power of population tests. It can also be seen that power increases with the number of Bootstrap replications, itself reducing the level of discretization. The type of Bootstrap, B-LOO versus B-0.632, does not change the power. Again, consistent with the observation that it is discretization that drives the power loss.

Name	Basis	Boot Type	B	Accuracy	Parameters
lda.Boot.1	LDA	B-0.632	10	accuracy	–
lda.Boot.2	LDA	B-LOO	10	accuracy	–
svm.Boot.1	SVM	B-0.632	10	accuracy	cost=1e1
svm.Boot.2	SVM	B-LOO	10	accuracy	cost=1e1
svm.Boot.3	SVM	B-0.632	50	accuracy	cost=1e1
svm.Boot.4	SVM	B-LOO	50	accuracy	cost=1e1

Table 2: The same as Table 1 for bootstraped accuracy estimates. B-LOO and B-0.632 are defined in definitions 1 and 2 respectively. B denotes the number of Bootstrap samples.

6.4   High dimensional classifiers

It is known that when $p > n$ Hotelling's T^2, and Fisher's LDA are not computable. In our simulations, in which $p = 23$ and $n = 40$ is "almost" high dimensional, but still allows to compute both tests. We have simulated two high dimensional versions of Hotelling's T^2: *sd* [Srivastava, 2007] and *Hotelling.shrink* [Schäfer and Strimmer, 2005]. The former solves the dimensionality problem by assuming independence over coordinates, and the latter by Tikhonov regularization of the covariance, a-la ridge regression. The corresponding high dimensional accuracy tests would be a *naive Bayes* classfier, and l_2 regularized SVM [Ramdas et al., 2016]. We conjecture that they would not alter our conclusions, since the main force driving the conservativism is discretization, which they do not solve.
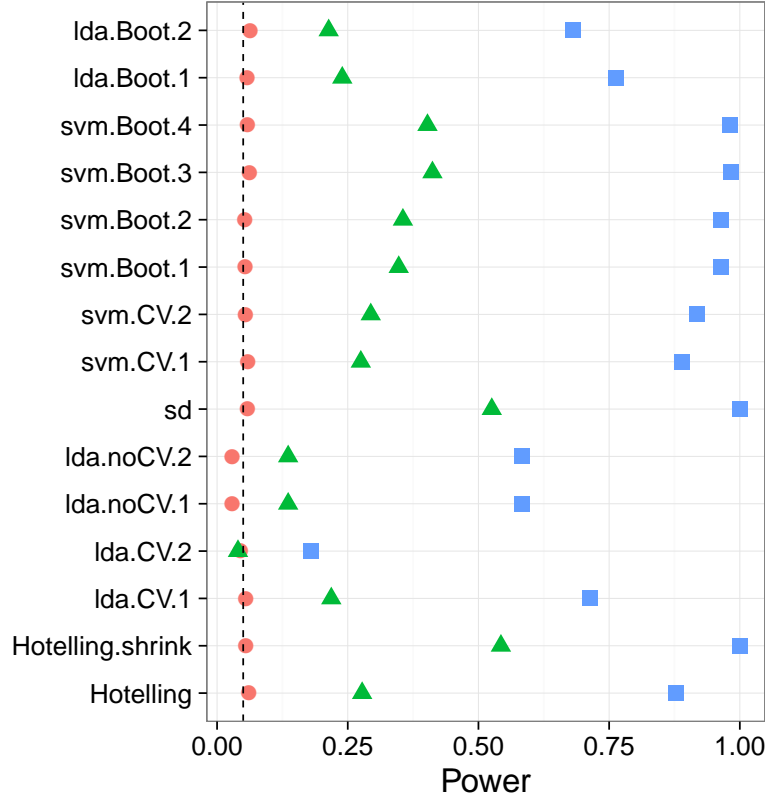
Figure 3: **Bootstrap:** *The power of a permutation test with various test statistics. The power on the x axis. Effect are color and shape coded. The various statistics on the y axis. Their details are given in tables 1 and 2. Effects vary over* 0 *(red circle),* 0.25 *(green triangle), and* 0.5 *(blue square). Simulation details in Appendix B.*

6.5   Related Literature

Olivetti et al. [2012] and Olivetti et al. [2014] looked into the problem of choosing a good accuracy test. They propose a new test they call an *independence test*, and demonstrate by simulation that it has more power than other accuracy tests, and can deal with non-balanced data sets. We did not include this test in the battery we compared, but we note the following: (a) The independence test of Olivetti et al. [2012] relies on a discrete test statistic. This means that in the cases that the accuracy test is called upon for discriminating populations, it will probably be underpowered compared to population tests. (b) In contrast with the underlying motivation of Olivetti et al. [2012]'s independence test, we did not find that balancing the data

13

folds is crucial for an accuracy test.

Golland et al. [2005] study accuracy tests using simulation, neuroimaging data, genetic data, and analytically. Their analytic results formalize our intuition from Section 1 on the effect of concentration of the accuracy statistic: The finite Vapnik–Chervonenkis (VC) dimension requirement [Golland and Fischl, 2003, Sec 4.3] prevents the permutation p-value from (asymptotically) concentrating. They also find that the power decreases with the level of discretization of the statistic. This is seen in their Figure 4, where the size of the test-set, K, governs the discretization. Since they permute features, and not labels, then all their permutation samples are balanced, and there is no issue of refolding.

Golland et al. [2005] simulate the power of an accuracy test using a multivariate Gaussian mixture, with a parameter p governing the separation between classes. Under their model $(x_i|y_i = 1) \sim p\mathcal{N}(\mu_1, I) + (1 - p)\mathcal{N}(\mu_2, I)$ and $(x_i|y_i = -1) \sim (1 - p)\mathcal{N}(\mu_1, I) + p\mathcal{N}(\mu_2, I)$. Varying p interpolates between the null distribution ($p = 0.5$) and a location shift model ($p = 0$). We perform the same simulation as Golland et al. [2005], after reparametrizing p so that $p = 0$ corresponds to the null model, and $p = 23$ to be comparable to our other simulations. We find that in this mixture class of models, like the location class of models, a population test has more power than an accuracy test (Figure 4).

6.6 Reservations

Some reservations to the generality of our findings are in order. Firstly, not all accuracy tests are concerned with signal detection. Consider brain decoding for machine interfaces, and clinical diagnosis, where the presence of a medical condition is predicted from imaging data [e.g. Olivetti et al., 2012, Wager et al., 2013]. In those examples, the purpose of the test is not to detect a difference between classes, but to actually test the performance of a particular classifier. As put by Ojala and Garriga [2010]:

> . . . these tests study whether the classifier is using the described properties and not whether the plain data contain such properties. For studying the characteristics of a population represented by the data, standard statistical test could be used.

This is because classification is harder than detection. We may be able to detect a difference between classes, but not be able to classify examples significantly better than chance.

Secondly, it may be argued that accuracy tests permits the separation between classes in high dimensions, such as in *reproducing kernel Hilbert*
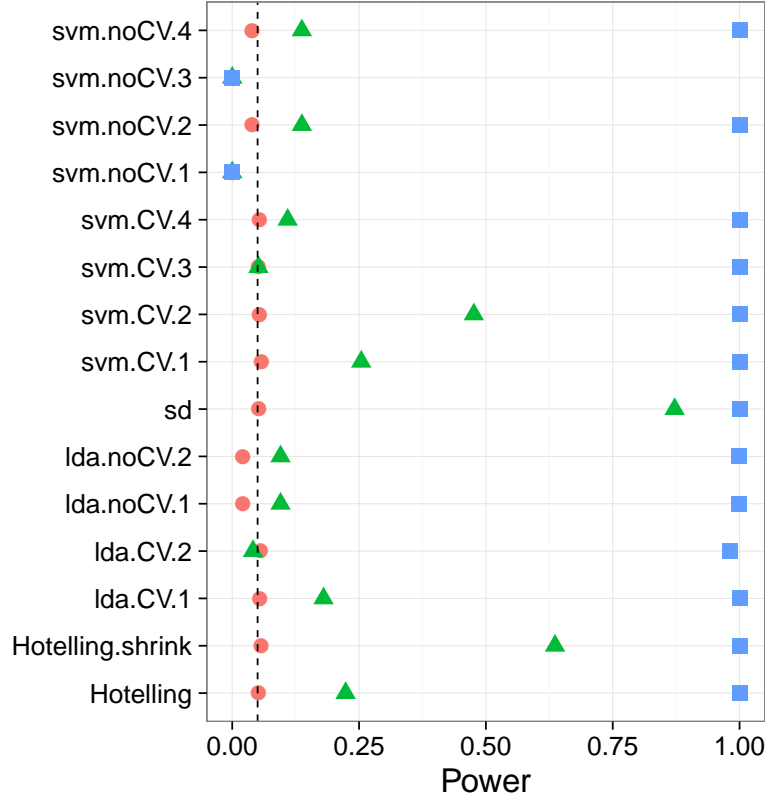
14

Figure 4: **Mixture:** $\mathbf{x}_i = \chi_i \mu + \eta_i; \chi_i = \{-1, 1\}$ and $Prob(\chi_i = 1) = (1/2 - p)^{\mathbf{y}_i^*}(1/2 + p)^{1 - \mathbf{y}_i^*}$. μ is a p-vector with $3/\sqrt{p}$ in all coordinates. The effect, p, is color and shape coded and varies over 0 (red circle), 1/4 (green tringle) and 1/2 (blue square).

spaces (RKHS) by using non-linear predictors. This is a false argument– accuracy test do not have any more flexibility that population tests. Indeed, it is possible to test for location in the same dimension the classifier is learned. Gretton et al. [2012] is an example where the test for location is performed in the RKHS of the data. It is also possible to test for the equality of two multivariate distributions without specifying any a-priori alternative [e.g. **?**]). On the other hand, based on our reported neuroimaging example, and others, we find that a population test in the original feature space is indeed a simple and powerful approach to signal detection.

6.7 Epilogue

Given all the above, we find the popularity of accuracy tests quite puzzling. We believe this is due to a reversal of the inference cascade. Researchers first fit a classifier, and then ask if the classes are any different. Were they to start by asking if classes are any different, and only then try to classify, then population tests would naturally arise as the preferred method. As put by Ramdas et al. [2016]:

> The recent popularity of machine learning has resulted in the extensive teaching and use of prediction in theoretical and applied communities and the relative lack of awareness or popularity of the topic of Neyman-Pearson style hypothesis testing in the computer science and related "data science" communities.

And more simply by Frank Harrell in the CrossValidated Q&A site[3]:

> ... your use of proportion classified correctly as your accuracy score. This is a discontinuous improper scoring rule that can be easily manipulated because it is arbitrary and insensitive.

7 Acknowledgments

---

[3]http://stats.stackexchange.com/questions/17408/
how-to-assess-statistical-significance-of-the-accuracy-of-a-classifier.

References

T. W. Anderson. *An Introduction to Multivariate Statistical Analysis*. Wiley-Interscience, Hoboken, NJ, 3 edition edition, July 2003. ISBN 978-0-471-36091-9.

Y. Benjamini and Y. Hochberg. Controlling the false discovery rate: a practical and powerful approach to multiple testing. *JOURNAL-ROYAL STATISTICAL SOCIETY SERIES B*, 57:289–289, 1995.

R. Gilron, J. Rosenblatt, O. Koyejo, R. A. Poldrack, and R. Mukamel. Quantifying spatial pattern similarity in multivariate analysis using functional anisotropy. *arXiv:1605.03482 [q-bio]*, May 2016.

P. Golland and B. Fischl. Permutation tests for classification: towards statistical significance in image-based studies. In *IPMI*, volume 3, pages 330–341. Springer, 2003.

P. Golland, F. Liang, S. Mukherjee, and D. Panchenko. Permutation Tests for Classification. In P. Auer and R. Meir, editors, *Learning Theory*, number 3559 in Lecture Notes in Computer Science, pages 501–515. Springer Berlin Heidelberg, June 2005. ISBN 978-3-540-26556-6 978-3-540-31892-7. doi: 10.1007/11503415_34.

T. R. Golub, D. K. Slonim, P. Tamayo, C. Huard, M. Gaasenbeek, J. P. Mesirov, H. Coller, M. L. Loh, J. R. Downing, M. A. Caligiuri, C. D. Bloomfield, and E. S. Lander. Molecular Classification of Cancer: Class Discovery and Class Prediction by Gene Expression Monitoring. *Science*, 286(5439):531–537, Oct. 1999. ISSN 0036-8075, 1095-9203. doi: 10.1126/science.286.5439.531.

A. Gretton, K. M. Borgwardt, M. J. Rasch, B. Schölkopf, and A. Smola. A Kernel Two-sample Test. *J. Mach. Learn. Res.*, 13:723–773, Mar. 2012. ISSN 1532-4435.

T. Hastie, R. Tibshirani, and J. Friedman. *The Elements of Statistical Learning*. Springer, July 2003. ISBN 0-387-95284-5.

J. Hemerik and J. Goeman. Exact testing with random permutations. *arXiv:1411.7565 [math, stat]*, Nov. 2014.

H. Hotelling. The Generalization of Student's Ratio. *The Annals of Mathematical Statistics*, 2(3):360–378, Aug. 1931. ISSN 0003-4851, 2168-8990. doi: 10.1214/aoms/1177732979.

W. Jiang, S. Varma, and R. Simon. Calculating confidence intervals for prediction error in microarray classification using resampling. *Statistical Applications in Genetics and Molecular Biology*, 7(1), 2008.

L. Juan and H. Iba. Prediction of tumor outcome based on gene expression data. *Wuhan University Journal of Natural Sciences*, 9(2):177–182, Mar. 2004. ISSN 1007-1202, 1993-4998. doi: 10.1007/BF02830598.

N. Kriegeskorte, R. Goebel, and P. Bandettini. Information-based functional brain mapping. *Proceedings of the National Academy of Sciences of the United States of America*, 103(10):3863–3868, July 2006. ISSN 0027-8424, 1091-6490. doi: 10.1073/pnas.0600244103.

E. L. Lehmann. Parametric versus nonparametrics: two alternative methodologies. *Journal of Nonparametric Statistics*, 21(4):397–405, 2009. ISSN 1048-5252. doi: 10.1080/10485250902842727.

G. J. McLachlan. The bias of the apparent error rate in discriminant analysis. *Biometrika*, 63(2):239–244, Jan. 1976. ISSN 0006-3444, 1464-3510. doi: 10.1093/biomet/63.2.239.

S. Mukherjee, P. Tamayo, S. Rogers, R. Rifkin, A. Engle, C. Campbell, T. R. Golub, and J. P. Mesirov. Estimating dataset size requirements for classifying DNA microarray data. *Journal of Computational Biology: A Journal of Computational Molecular Cell Biology*, 10(2):119–142, 2003. ISSN 1066-5277. doi: 10.1089/106652703321825928.

M. Ojala and G. C. Garriga. Permutation Tests for Studying Classifier Performance. *Journal of Machine Learning Research*, 11(Jun):1833–1863, 2010. ISSN ISSN 1533-7928.

E. Olivetti, S. Greiner, and P. Avesani. Induction in Neuroscience with Classification: Issues and Solutions. In G. Langs, I. Rish, M. Grosse-Wentrup, and B. Murphy, editors, *Machine Learning and Interpretation in Neuroimaging*, number 7263 in Lecture Notes in Computer Science, pages 42–50. Springer Berlin Heidelberg, 2012. ISBN 978-3-642-34712-2 978-3-642-34713-9. doi: 10.1007/978-3-642-34713-9_6.

E. Olivetti, S. Greiner, and P. Avesani. Statistical independence for the evaluation of classifier-based diagnosis. *Brain Informatics*, 2(1):13–19, Dec. 2014. ISSN 2198-4018, 2198-4026. doi: 10.1007/s40708-014-0007-6.

18

F. Pereira, T. Mitchell, and M. Botvinick. Machine learning classifiers and fMRI: A tutorial overview. *NeuroImage*, 45(1, Supplement 1):S199–S209, Mar. 2009. ISSN 1053-8119. doi: 10.1016/j.neuroimage.2008.11.007.

C. R. Pernet, P. McAleer, M. Latinus, K. J. Gorgolewski, I. Charest, P. E. G. Bestelmeyer, R. H. Watson, D. Fleming, F. Crabbe, M. Valdes-Sosa, and P. Belin. The human voice areas: Spatial organization and inter-individual variability in temporal and extra-temporal cortices. *NeuroImage*, 119:164–174, Oct. 2015. ISSN 1053-8119. doi: 10.1016/j.neuroimage.2015.06.050.

M. D. Radmacher, L. M. McShane, and R. Simon. A Paradigm for Class Prediction Using Gene Expression Profiles. *Journal of Computational Biology*, 9(3):505–511, June 2002. ISSN 1066-5277. doi: 10.1089/106652702760138592.

A. Ramdas, A. Singh, and L. Wasserman. Classification Accuracy as a Proxy for Two Sample Testing. *arXiv:1602.02210 [cs, math, stat]*, Feb. 2016.

J. Schäfer and K. Strimmer. A Shrinkage Approach to Large-Scale Covariance Matrix Estimation and Implications for Functional Genomics. *Statistical Applications in Genetics and Molecular Biology*, 4(1), Jan. 2005. ISSN 1544-6115. doi: 10.2202/1544-6115.1175.

D. K. Slonim, P. Tamayo, J. P. Mesirov, T. R. Golub, and E. S. Lander. Class Prediction and Discovery Using Gene Expression Data. In *Proceedings of the Fourth Annual International Conference on Computational Molecular Biology*, RECOMB '00, pages 263–272, New York, NY, USA, 2000. ACM. ISBN 978-1-58113-186-4. doi: 10.1145/332306.332564.

M. S. Srivastava. Multivariate Theory for Analyzing High Dimensional Data. *Journal of the Japan Statistical Society*, 37(1):53–86, 2007. doi: 10.14490/jjss.37.53.

M. S. Srivastava, S. Katayama, and Y. Kano. A two sample test in high dimensional data. *Journal of Multivariate Analysis*, 114:349–358, Feb. 2013. ISSN 0047-259X. doi: 10.1016/j.jmva.2012.08.014.

J. Stelzer, Y. Chen, and R. Turner. Statistical inference and multiple testing correction in classification-based multi-voxel pattern analysis (MVPA): Random permutations and cluster size control. *NeuroImage*, 65:69–82, Jan. 2013. ISSN 1053-8119. doi: 10.1016/j.neuroimage.2012.09.063.

477 A. W. van der Vaart. *Asymptotic Statistics*. Cambridge University Press,
478 Cambridge, UK ; New York, NY, USA, Oct. 1998. ISBN 978-0-521-49603-
479 2.

480 G. Varoquaux, P. R. Raamana, D. Engemann, A. Hoyos-Idrobo, Y. Schwartz,
481 and B. Thirion. Assessing and tuning brain decoders: cross-validation,
482 caveats, and guidelines. working paper or preprint, June 2016.

483 T. D. Wager, L. Y. Atlas, M. A. Lindquist, M. Roy, C.-W. Woo, and E. Kross.
484 An fMRI-Based Neurologic Signature of Physical Pain. *New England Jour-*
485 *nal of Medicine*, 368(15):1388–1397, Apr. 2013. ISSN 0028-4793. doi:
486 10.1056/NEJMoa1204471.

A Analysis pipeline

Here is the analysis pipeline of Stelzer et al. [2013] we for the auditory data in Gilron et al. [2016]. Denoting by $i = 1, \ldots, I$ the subject index, $v = 1, \ldots, V$ the voxel index, and $s = 1, \ldots, S$ the permutation index. Since regions[4] are centered around a unique voxel, the voxel index v also serves as a unique region index. Algorithm 1 computes a region-wise test statistic, which is compared to its permutation null distribution computed by Algorithm 2.

Algorithm 1: Compute a group parametric map.

Data: fMRI scans, and experimental design.
Result: Brain map of group statistics: $\{\bar{T}_v\}_{v=1}^V$

1 **for** $v \in 1, \ldots, V$ **do**
2   **for** $i \in 1, \ldots, I$ **do**
3        $T_{i,v} \leftarrow$ test statistic for subject i in a region centered at v.
4     $\bar{T}_v \leftarrow \frac{1}{I} \sum_{i=1}^I T_{i,v}$.

Algorithm 2: Compute a permutation p-value map.

Data: fMRI scans of 20 subjects, experimental design.
Result: Brain map of permutation p-values: $\{p_v\}_{v=1}^V$

1 **for** $s \in 1, \ldots S$ **do**
2   permute labels;
3     $\bar{T}_v^s \leftarrow$ parametric map

---

[4]*searchlight* or *sphere* in the MVPA parlance

B Simulation Details

The follwing details are common to all the reported simulations, unless stated otherwise in a figure's caption. The R code for the simulations can be found in [TODO].

Each simulation is based on $4,000$ replications. In each replication, we generate n i.i.d. samples from a shift model $\mathbf{x}_i = \mu \mathbf{y}_i^* + \eta_i$. Where $y_i^* = \{0, 1\}$ is the class of subject i in dummy coding. Recalling that $y_i = \{-1, 1\}$ is the class in effect coding, then clearly $y_i = 2y_i^* - 1$. The noise is distributed as $\eta_i \sim \mathcal{N}_p(0, \Sigma)$. The sample size $n = 40$. The dimension of the data is $p = 23$. The covariance $\Sigma = I$. Effects, i.e. shifts μ, are equal coordinate p-vectors with coordinates that vary over $\mu \in \{0, 1/4, 1/2\}$.

Having generated the data, we compute each of the test statistics in Table 1. For test statistics that require data folding, we used 8 folds. We then compute a permutation p-value by permuting the class labels, and recomputing each test statistic. We perform 400 such permutations. We then reject the $\mu_i = 0$ null hypothesis if the permutation p-value is smaller than 0.05. The reported power is the proportion of replication where the permutation p-value falls below 0.05.

C Simulation Results

Figure 5: Simulation details in Appendix B except the changes in the sub-captions.

(a) 2-fold cross validation.
Balanced folding.

(b) 20-fold cross validation.
Balanced folding

Figure 6: *Simulation details in Appendix B except the changes in the sub-captions.*
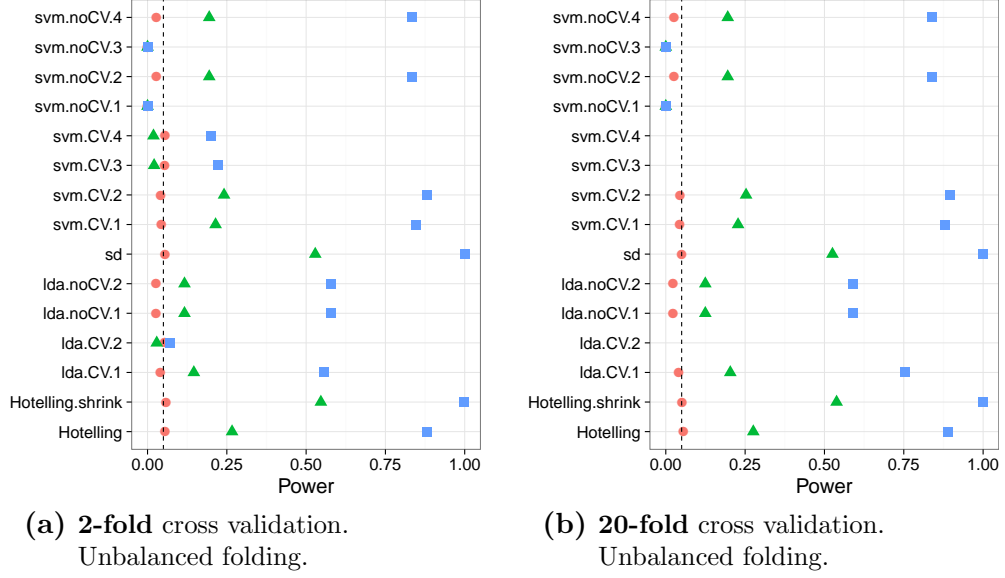
(a) 2-fold cross validation. Unbalanced folding.

(b) 20-fold cross validation. Unbalanced folding.

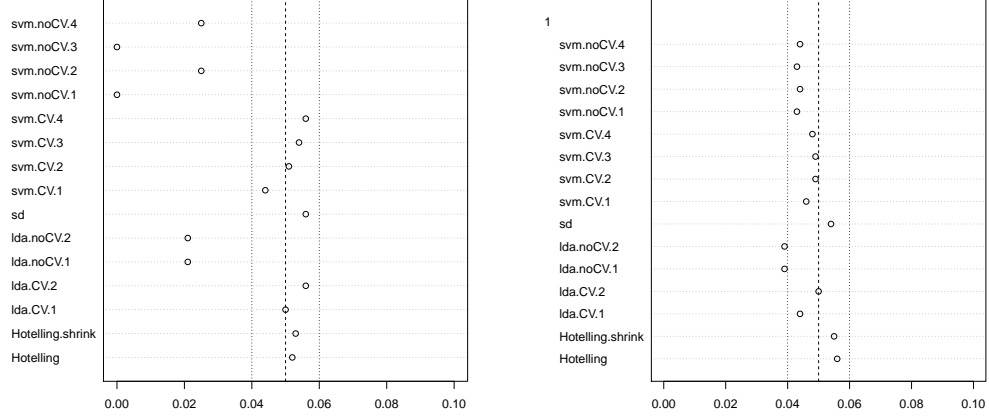Figure 7: *Simulation details in Appendix B except the changes in the sub-captions.*

(a) Scale Change: $\mathbf{x}_i = \eta_i * \mu^{\mathbf{y}_i^*}$ so that the effect are a scale change.

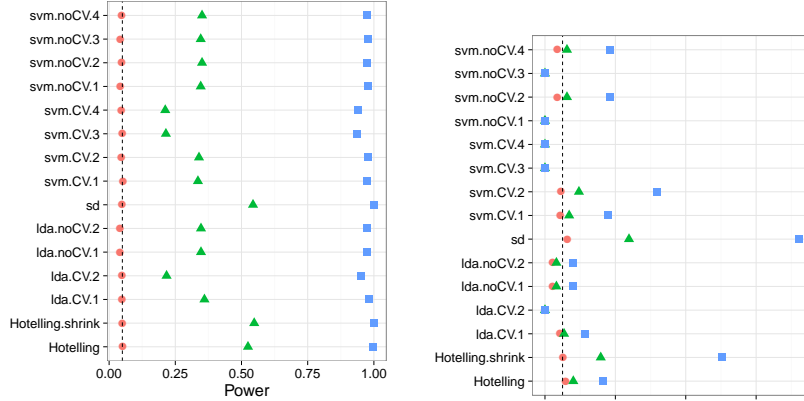**(b) Heavytailed:** η_i is not *p*-variate Gaussian, but rather *p*-variate t, with $df = 3$.

Figure 8: Simulation details in Appendix B except the changes in the sub-captions.

(a) **Low-Dimension:** False positive rates for $n = 40$.

(b) **High-Dimension:** False positive rates for $n = 400$.

Figure 9: Simulation details in Appendix B except the changes in the sub-captions.

(a) **High-Dimension, local alternative:** $n = 400$, $\mu \in \frac{1}{\sqrt{10}} \times \{0, 1/4, 1/2\}$.

(b) **AR(1) dependence:** $\Sigma_{k,l} = \rho^{|k-l|}; \rho = 0.8$.